



INTEGRAL ENERGY EQUATION MODEL FOR HEAT CONVECTION TO TURBULENT BOUNDARY LAYER ON A FLAT PLATE

Mohammad Hasan Khademi^{a*} and Abbas Mozafari^b

^a Department of Chemical Engineering, Faculty of Engineering, University of Isfahan, 81746-73441, Isfahan, Iran

^b Chemical Engineering Department, Shahrood Branch, Islamic Azad University, Shahrood, Iran

ABSTRACT

An integral energy equation model is used to calculate the heat transfer coefficient/Nusselt number, thermal boundary layer thickness and temperature distribution in the turbulent boundary layer for forced convection over a smooth flat plate. The proposed model is based on two polynomial temperature profiles in a thermal laminar sublayer as well as in a fully developed boundary layer and two integral energy equations. The performance of this new model is compared with the most commonly used semi-empirical correlations and the complex established models such as $k-\varepsilon$, $k-\omega$, RSM, and a good agreement is achieved.

Keywords: Turbulent boundary layer; integral energy equation; heat transfer coefficient; flat plate.

1. INTRODUCTION

Turbulence modeling is the construction and use of a model to predict the effects of turbulence, and divided into three general categories:

- 1) The most natural and straight forward approach to turbulence simulations is to solve the Navier-Stokes equations without any approximation of the turbulence other than numerical discretization. This type of simulation is called *Direct Numerical Simulation* (DNS). In such simulations all the motions contained in the flows are resolved. In order to capture the structures of the turbulence one have to use extremely fine grids and time steps for these type of simulations. Due to this, DNS is very costly from a computational point of view and this method is only useful for flows with low Reynolds numbers. The application of DNS is therefore limited to turbulence research and results from DNS simulations can be important to verify results from other turbulence models.
- 2) A simulation that is less computationally costly is *Large Eddy Simulation* (LES). This type of simulation uses the fact that the large scale motions are generally more energetic than the small scale ones. These large eddies are more effective transporters of the conserved properties and therefore LES treats the large eddies more exactly than the small scale ones. LES is preferred over DNS when the Reynolds number is too high or the computational domain is too complicated.
- 3) Both DNS and LES modeling give a detailed description of turbulent flows. If one is not interested in that much details of the turbulence, a *Reynolds-Averaged Navier-Stokes* model (RANS model) can be a good choice. This type of model is much less costly compared to both DNS and LES. In the RANS approach to turbulence, all of the unsteadiness in the flow is averaged out and regarded as part of the turbulence. When averaging, the non-linearity of the Navier-Stokes equations gives rise to terms that must be modeled. These terms can be modeled differently leading to various types of RANS models, each behaving differently

depending on the Reynolds number of the flow, the computational domain, and etc. The various RANS models are classified in terms of number of transport equations solved:

- a) Zero-equation model; mixing length model (Van Driest, 1956).
- b) One-equation models; Prandtl's one-equation model (Glushko, 1965), Baldwin-Barth model (1990), Spalart-Allmaras model (1994).
- c) Two-equation models; $k-\varepsilon$ style models contains standard $k-\varepsilon$ (Launder and Sharma, 1974), RNG $k-\varepsilon$ (Yakhot *et al.*, 1992), etc., $k-\omega$ models contains Wilcox $k-\omega$ (Wilcox, 1988), SST $k-\omega$ (Menter, 1994), etc.
- d) Nonlinear eddy viscosity models; v^2-f model (Popovac and Hanjalic, 2007).
- e) Reynolds Stress Model (RSM) (Launder *et al.*, 1975).

These models attempt to predict turbulence by two or more partial differential equations (PDEs) so; they are in general much complicate and contain many parameters. However, they are much expensive in terms of memory as they require two/more extra PDEs. Therefore, the lack of a simple model to predict accurately turbulent flow is felt.

External forced convection heat transfer from isothermal or isoflux external flat surfaces is an important problem for engineers. There are many engineering systems that are modeled using forced convection, such as plate type heat exchanger design.

There have been a number of studies on the heat transfer characteristics of turbulent flow over flat plate. Wassel and Catton (1973) investigated three different hypotheses representing turbulent transport on a flat plate, namely, the Van Driest model (1956) of turbulence, a modified Nee-Kovaszny (1969) hypothesis and a combination of the kinetic energy of turbulence and the mixing length hypotheses; and developed a model for the variable turbulent Prandtl number. Chung and Sung (1984) analyzed numerically turbulent convective heat transfer with appreciable buoyancy effect over a heated or cooled horizontal flat plate by solving four equations for mean square temperature variance $\overline{\theta^2}$, its rate of destruction ε_θ , turbulent kinetic energy k and the rate of

* Corresponding author. Email: m.khademi@eng.ui.ac.ir

kinetic energy dissipation ε . A Heat transfer and dispersion model for both laminar and turbulent regimes in flat plate heat exchangers were considered by Pinson *et al.* (2007). The velocity and thermal laws of the wall and wake were used by Sucec (2006), in modern integral methods for turbulent boundary layer, to solve the momentum and thermal energy equations in their integral forms to give predictions of the Stanton number distribution. Vallejo and Trevino (1990) analyzed the cooling of a flat plate in a convective flow, taking into account the longitudinal heat conduction through the plate. Both laminar and turbulent boundary layer flows were considered and the three term asymptotic solution was compared with the numerical solution of the governing equation. Kondjoyan *et al.* (2004) described the effect of highly turbulent air flows on the development of a flat-plate boundary layer at Reynolds numbers ranging from 8400 to 127000. Radmehr and Patankar (2001) proposed two independent solution approaches to compute the transition boundary layer using low-Reynolds-number turbulence models: (1) to solve the boundary layer equations over a flat plate with the starting location of calculation very close to the leading edge of the plate, and (2) to solve the elliptic Navier–Stokes equations over the whole plate, including the leading edge and some region upstream of it. Ilegbusi (1989) described the calculation of a turbulent boundary layer on a porous flat plate with severe injection at different rates and at different angles to the surface using two turbulent models, namely, the $k-\omega$ (Ilegbusi and Spalding, 1989) and $k-\varepsilon$ (Launder and Spalding, 1974) models. Various comparisons among well-known equations of the convection heat transfer coefficient and those that

come from the boundary layer theory for forced air flow over flat surfaces and particularly over flat plate solar collectors, with the aim at arriving at a consensus on which of such equations is more accurate, are carried out by Sartori (2006).

Also, several attempts have been made over the years to develop generalized Nusselt number correlations that would apply to a range of Reynolds and Prandtl numbers. Table 1 summarizes some of these correlations for the turbulent flow on a flat plate.

In the present study, a new relatively simple model is proposed to investigate the turbulent flow of water and air over a flat plate with constant surface temperature. This model is based on two polynomial temperature profiles in a thermal laminar sublayer as well as in a fully developed boundary layer and two integral energy equations. This approximate method is even easy to implement. Such model can approximate the governing PDEs to ordinary differential equations (ODEs), which leads to reduce the computer runtime. This method, however, involves a lot of embedded empiricism not only in turbulent modeling but in closing the integral equations. The evolution of thermal boundary layer thickness, temperature profile and heat transfer coefficient inside the turbulent boundary layer on the flat plate is calculated using this new model. The Nusselt number that comes from this integral energy equations model is compared with the semi-empirical correlations shown in Table 1 and the complex models such as $k-\varepsilon$, $k-\omega$, RSM, with the aim at detecting validation.

Table 1: Common semi-empirical correlations of Nusselt number for the turbulent boundary layer on a flat plate.

Formula	Validity	Ref.	Eq.
$Nu_x = 0.0296Re_x^{4/5}Pr^{1/3}$	$5 \times 10^5 < Re_x < 10^7$ $0.6 < Pr < 60$	Schlichting (1968)	(1)
$Nu_x = \frac{0.0288Re_x^{0.8}Pr}{1 + 0.849Re_x^{-0.1} \left\{ (Pr-1) + \ln \left[\frac{5Pr+1}{6} \right] \right\}}$		Pitts and Sissom (1997)	(2)
$Nu_x = 0.032Re_x^{0.8}Pr^{0.43}$	$2 \times 10^5 < Re_x < 5 \times 10^6$	Zukauskas and Slanciauskas (1987)	(3)
$Nu_x = \frac{C_f}{2} \frac{1}{1 + 5(Pr-1) \sqrt{\frac{C_f}{2}}}$		Baehr and Stephan (2006)	(4)
$Nu_x = 0.45 + \left(0.3387\varphi^{1/2} \right) \left\{ 1 + \frac{(\varphi/2600)^{3/5}}{[1 + (\varphi_u/\varphi)^{7/2}]^{2/5}} \right\}^{1/2}$	$10^5 < \varphi_u < 10^7$	Churchill (1976)	(5)
$\varphi = Re_x Pr^{2/3} \left[1 + \left(\frac{0.0468}{Pr} \right)^{2/3} \right]^{-1/2}$			
$Nu_x = 0.185(\log Re_x)^{-2.584} Re_x Pr^{1/3}$	$10^7 < Re_x < 10^9$	Holman (1989)	(6)

2. MODEL DESCRIPTION

For incompressible flow along a flat plate, the energy equation is expressed in terms of the following turbulent boundary layer equation:

$$(\bar{v} + v') \frac{\partial(\bar{T} + T')}{\partial y} + (\bar{u} + u') \frac{\partial(\bar{T} + T')}{\partial x} = \alpha \frac{\partial^2(\bar{T} + T')}{\partial y^2} + \frac{\mu}{\rho C_p} \left(\frac{\partial(\bar{u} + u')}{\partial y} \right)^2 \quad (7)$$

To construct the model, an approximate analysis which furnishes an easier solution is used without a loss in physical understanding of the processes. To simplify the analysis, the following assumptions are considered:

- The fluid is incompressible, and the flow is steady.
- The free-stream temperature and velocity are constant.
- The fluctuation in velocity and temperature is neglected.
- The fluid physical properties are assumed constant and are calculated at the average temperature of wall and fluid (film temperature).
- There is no pressure variation in the direction perpendicular to the plate.
- The turbulent zone starts at the end of laminar zone; the transition zone is neglected. As, Shames (2003) was noted that the transition occurs in the range of $Re = 3.2 \times 10^5$ to 10^6 . In addition, he was noted that cannot prescribe a specific Reynolds number for transition because of the effect of many factors that are involved in the transition process. The high value of 10^6 can be reached by

having very small turbulence, plate smoothness, and so on. So, in this study similar to the shames work, the value of 5×10^5 is generally used as the critical Reynolds number Re_{cr} .

- The stream-wise pressure gradient is neglected.
- As the buffer zone is a transient region from laminar sublayer to turbulent boundary layer zone so, that is neglected.

Figure 1 shows a schematic of a thermal boundary layer flow system consists of laminar and turbulent zone. In the turbulent zone, the thermal laminar sublayer thickness is δ_{t1} , the thermal fully developed turbulent boundary layer thickness is δ_{t2} , the wall temperature is T_w , and the free-stream temperature and velocity outside the turbulent boundary layer is T_∞ and u_∞ , respectively.

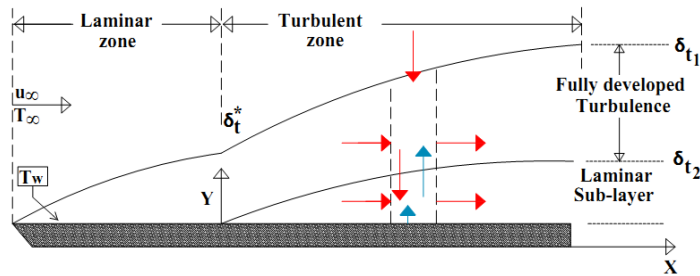


Fig. 1 A schematic of a thermal boundary layer flow system (red arrow: heat convection; blue arrow: heat conduction).

Two total energy balances are applied on the control volume shown in Fig. 1. These two integral energy equations become:

$$\rho C_p \frac{d}{dx} \int_0^{\delta_{t1}} (T_1 - T_2) u_1 dy + \rho C_p \left. \frac{dT_2}{dx} \right|_{y=\delta_{t1}} \int_0^{\delta_{t1}} u_1 dy + k \left. \frac{\partial T_1}{\partial y} \right|_{y=0} - k \left. \frac{\partial T_1}{\partial y} \right|_{y=\delta_{t1}} - \mu \int_0^{\delta_{t1}} \left(\frac{du_1}{dy} \right)^2 dy = 0 \quad (8)$$

$$\rho C_p \frac{d}{dx} \int_{\delta_{t1}}^{\delta_{t2}} (T_2 - T_\infty) u_2 dy + \rho C_p \frac{d}{dx} \int_0^{\delta_{t1}} (T_2 - T_\infty) u_1 dy - \rho C_p \left. \frac{dT_2}{dx} \right|_{y=\delta_{t1}} \int_0^{\delta_{t1}} u_1 dy + k \left. \frac{\partial T_1}{\partial y} \right|_{y=\delta_{t1}} - \int_{\delta_{t1}}^{\delta_{t2}} E_\mu \left(\frac{du_2}{dy} \right)^2 dy = 0 \quad (9)$$

The details of calculation of these two equations are given in appendixes A and B.

Khademi *et al.* (2010) analyzed a simple model for turbulent boundary layer momentum transfer on a flat plate. This model can be used to calculate the velocity profiles in the laminar sublayer and fully developed turbulent boundary layer zones, u_1 and u_2 . If the temperature profiles were known, the appropriate functions alongside u_1 and u_2 (calculated by Khademi *et al.* (2010)) could be inserted in Eqs. (8) and (9) to obtain two expressions for the thermal boundary layer thicknesses. The details of momentum transfer equations are presented by Khademi *et al.* (2010).

For the proposed approximate analysis method, some boundary conditions are first written down that the temperature functions must satisfy:

$$T_1 = T_w \quad \text{at } y = 0 \quad (10)$$

$$T_1 = T_2 \quad \text{at } y = \delta_{t1} \quad (11)$$

$$k \frac{\partial T_1}{\partial y} = (k + E_T) \frac{\partial T_2}{\partial y} \quad \text{at } y = \delta_{t1} \quad (12)$$

$$T_2 = T_\infty \quad \text{at } y = \delta_{t2} \quad (13)$$

$$\frac{\partial T_2}{\partial y} = 0 \quad \text{at } y = \delta_{t2} \quad (14)$$

With disregarding viscous heating, Eq. (7) yields:

$$\frac{\partial^2 T_1}{\partial y^2} = 0 \quad \text{at } y = 0 \quad (15)$$

Since the velocities u and v are zero at $y = 0$.

The temperature profiles at various x positions are assumed to be similar; that is, they have the same functional dependence on the y coordinate. The simplest functions that it can be chosen to satisfy these boundary conditions are two polynomials with six arbitrary constants. Thus

$$T_1 = a_{t0} + a_{t1}y + a_{t2}y^2 + a_{t3}y^3 \quad (16)$$

$$T_2 = b_{t1}y + b_{t2}y^2 \quad (17)$$

T_1 and T_2 are temperature profiles in the laminar sublayer and fully developed turbulent zones, respectively.

These six boundary conditions (10) to (15) are applied in the polynomial functions (16) and (17), and then, the six arbitrary constants are calculated as follows:

$$a_{t0} = T_w \quad (18)$$

$$a_{t1} = \frac{T_\infty}{\delta_{t2}} \left(2 - \frac{E_T}{k} \right) - \frac{T_\infty \delta_{t1}}{\delta_{t2}^2} \left(\frac{1}{2} - \frac{E_T}{k} \right) - \frac{3T_w}{2\delta_{t1}} \quad (19)$$

$$a_{t2} = 0 \quad (20)$$

$$a_{t3} = \frac{T_\infty}{\delta_{t2} \delta_{t1}^2} \left(\frac{E_T}{k} \right) - \frac{T_\infty}{\delta_{t1} \delta_{t2}^2} \left(\frac{1}{2} + \frac{E_T}{k} \right) + \frac{T_w}{2\delta_{t1}^3} \quad (21)$$

$$b_{t1} = \frac{2T_w}{\delta_{t2}} \quad (22)$$

$$b_{t2} = \frac{-T_w}{\delta_{t2}^2} \quad (23)$$

According to Prandtl's mixing-length theory (Prandtl and Angew, 1925), the mixing length is proportional to the distance y measured from the solid surface. Correspondingly, the following form for the eddy thermal conductivity is suggested:

$$E_T = \rho C_p (\kappa y)^2 \frac{\partial u_2}{\partial y} \quad (24)$$

Here, κ is a universal constant whose value is given as 0.40 by some investigators and as 0.36 by others.

The proposed polynomial functions for the temperature profile in this paper and velocity distribution produced by Khademi *et al.* (2010) are inserted into Eqs. (8) and (9), and integrated. The result is two differential equations as below:

$$\rho C_p \frac{d}{dx} \left[a_{t0} a_1 \frac{\delta_{t1}^2}{2} + a_1 (a_{t1} - b_{t1}) \frac{\delta_{t1}^3}{3} + (a_{t0} a_3 - a_1 b_{t2}) \frac{\delta_{t1}^4}{4} + a_3 (a_{t1} - b_{t1}) \frac{\delta_{t1}^5}{5} - a_3 b_{t2} \frac{\delta_{t1}^6}{6} + a_3 a_{t3} \frac{\delta_{t1}^7}{7} \right] + \rho C_p \left(a_1 \frac{\delta_{t1}^2}{2} + a_3 \frac{\delta_{t1}^4}{4} \right) \frac{d}{dx} (b_{t1} \delta_{t1} + b_{t2} \delta_{t1}^2) - 3k a_{t3} \delta_{t1}^2 - \mu \left(a_1^2 \delta_{t1} + 2a_1 a_3 \delta_{t1}^3 + \frac{9}{5} a_3^2 \delta_{t1}^5 \right) = 0 \quad (25)$$

$$\rho C_p \frac{d}{dx} \left[\frac{-b_1 T_\infty}{2} (\delta_{t2}^2 - \delta_{t1}^2) + \frac{b_1 b_{t1} - b_2 T_\infty}{3} (\delta_{t2}^3 - \delta_{t1}^3) - a_1 T_\infty \frac{\delta_{t1}^2}{2} + \frac{b_1 b_{t2} + b_2 b_{t1}}{4} (\delta_{t2}^4 - \delta_{t1}^4) + \frac{b_2 b_{t2}}{5} (\delta_{t2}^5 - \delta_{t1}^5) + a_1 b_{t1} \frac{\delta_{t1}^3}{3} + (a_1 b_{t2} - a_3 T_\infty) \frac{\delta_{t1}^4}{4} + a_3 b_{t1} \frac{\delta_{t1}^5}{5} + a_3 b_{t2} \frac{\delta_{t1}^6}{6} \right]$$

$$\begin{aligned}
 &+k(a_{t1} + 3a_{t3}\delta_{t1}^2) - \rho\kappa^2 \left[\frac{b_1^3}{3}(\delta_{t2}^3 - \delta_{t1}^3) + \frac{3b_2b_1^2}{2}(\delta_{t2}^4 - \delta_{t1}^4) + \right. \\
 &\left. \frac{12b_1b_2^2}{5}(\delta_{t2}^5 - \delta_{t1}^5) + \frac{4b_2^3}{3}(\delta_{t2}^6 - \delta_{t1}^6) \right] \\
 &-\rho C_p \left(a_1 \frac{\delta_{t1}^2}{2} + a_3 \frac{\delta_{t1}^4}{4} \right) \frac{d}{dx} (b_{t1}\delta_{t1} + b_{t2}\delta_{t1}^2) = 0 \quad (26)
 \end{aligned}$$

where a_1, a_3, b_1 and b_2 are constants of polynomial functions of velocity profiles in viscous sublayer and fully developed turbulent zones, which is presented by khademi *et al.* (2010) in details.

Two following boundary conditions are needed to solve these two differential equations.

$$\delta_{t1} = 0 \quad \text{at } x = \frac{\mu Re_{cr}}{\rho u_\infty} \quad (27)$$

$$\delta_{t2} = \delta_t^* \quad \text{at } x = \frac{\mu Re_{cr}}{\rho u_\infty} \quad (28)$$

where δ_t^* is the boundary layer thickness of laminar flow at $Re_{cr} = 5 \times 10^5$.

3. NUMERICAL SOLUTION

An approximate method based on the integral energy equation followed by the numerical solution is used to obtain the thermal boundary layer thickness and temperature profile. Two ODEs (25) and (26) are solved simultaneously with their boundary conditions (Eqs. (27) and (28)). At first, these two equations (25) and (26) are rearranged in the form of $d\delta_1/dx = f(\delta_1, \delta_2)$ and $d\delta_2/dx = f(\delta_1, \delta_2)$ in the Maple programming environment. Then, these two last ODEs are solved by fourth order Runge-Kutta method which leads to obtaining δ_1 and δ_2 as a function of x . Since temperature profiles in laminar sub-layer and fully developed boundary-layer are functions of δ_1 and δ_2 , therefore these temperature profiles are obtained as functions of x and y .

4. RESULTS AND DISCUSSION

In this section, to verify the validity of this new model, the effect of various parameters such as Reynolds number, Prandtl number, free-stream velocity and wall to free-stream temperature ratio on the turbulent flow over a flat plate is analyzed in the boundary layer zone.

4.1 Heat transfer coefficient

The heat transfer coefficient could be calculated using the results obtained by this model. For this purpose, according to definition of heat transfer coefficient (Eq. (29)), the following relation (Eq. (30)) is obtained:

$$h = \frac{-k \frac{\partial T}{\partial y} \Big|_{y=0}}{T_w - T_\infty} \quad (29)$$

$$h = \frac{T_\infty}{T_w - T_\infty} \left[\frac{1}{\delta_{t2}} (E_T - 2k) + \frac{\delta_{t1}}{\delta_{t2}^2} \left(\frac{k}{2} - E_T \right) + \frac{3kT_w}{2T_\infty \delta_{t1}} \right] \quad (30)$$

Variation of the Nusselt number for air and water at free-stream velocity and temperature 5 m/s and 25 °C, respectively, and $T_w/T_\infty = 3$ along the flat plate (Reynolds number) is shown in Fig. 2. The Nusselt number increases with the Reynolds number on a logarithmic scale. In other word, the heat transfer coefficient decreases with the distance from the leading edge as a result of increasing in the turbulent boundary layer thickness. The Nusselt number calculated by the proposed model is compared with three different correlations, Eqs. (1), (4) and (5), as well as three complex models, $k-\epsilon$, $k-\omega$, and RSM. As illustrated in Fig. 2(a), for air at $Pr = 0.7$, the Nusselt number calculated by the proposed model is in good agreement with Eqs. (1) and (4) in the whole range of

the Reynolds numbers $5 \times 10^5 - 10^7$, and with Eq. (5) in the relatively high Reynolds numbers $> 5 \times 10^6$. However, the highest deviation between the present model and Eq. (5) appears at $Re = 5 \times 10^5$ with relative error 84%. As seen in Fig. 1, significant differences between the results of semi-empirical correlations and $k-\epsilon$, $k-\omega$, and RSM models are founded for air flow. The relative error between our model and these established models is 54% at $Re = 5 \times 10^5$, and 42% at $Re = 10^7$.

Figure 2(b) shows a good agreement between the present model for water at $Pr = 3.7$ and Eq. (5), and the $k-\epsilon$, $k-\omega$, and RSM models in the high Reynolds number $> 3 \times 10^6$ and to Eq. (4) in the low Reynolds number $< 3 \times 10^6$. In other word, the Nusselt number obtained by the present model starts to deviate from Eqs. (4), (5) and the complex established models at $Re = 3 \times 10^6$. The maximum deviation 46% occurs between such model and Eq. (4) at $Re = 10^7$, and 72% between that and Eq. (5) at $Re = 5 \times 10^5$. The average deviation between the proposed model and Eq. (1) is relatively within 30%. The highest relative error between this new model and the $k-\epsilon$, $k-\omega$, and RSM models is 50% at $Re = 5 \times 10^5$ which can be due to chosen boundary condition for laminar sub-layer thickness at the beginning of turbulent flow.

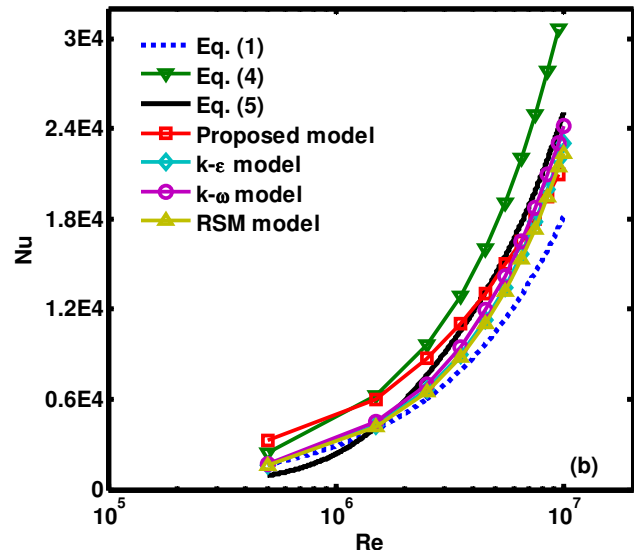
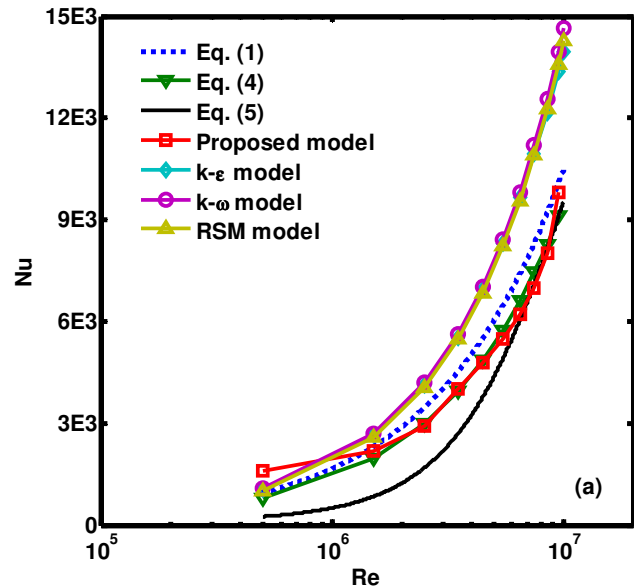


Fig. 2 Variation of the Nusselt number for (a) air and (b) water at $u_\infty = 5$ m/s, $T_\infty = 25$ °C, and $T_w/T_\infty = 3$ along the flat plate.

4.2 Influence of free-stream velocity

Figure 3(a) and (b) shows influence of the free-stream velocity on the laminar viscous sublayer thickness of water and turbulent boundary layer thickness of air, respectively, along the flat plate at $T_w/T_\infty = 3$ and free-stream temperature 25 °C. In Fig. 3(a) at constant free-stream velocity, the laminar sublayer thickness grows very slowly with a constant slope from the leading edge distance, whereas in Fig. 3(b), the turbulent boundary layer thickness continues this trend with more slopes. At any x position, the laminar sublayer and turbulent boundary layer thicknesses decrease as a result of increasing the free-stream velocity. In other word, both boundary layers shift to the down with the free-stream velocity. The plate role in terms of transport phenomena viewpoints is to inject the negative momentum to the flow. Increasing free-stream velocity results in a reduction in residence time. As a result, the net momentum injected to the flow by the plate decreases tending to a reduction in boundary layer thickness.

According to the Fig. 3(a) and (b), increasing the free-stream velocity from 5 to 15 m/s results in decreasing the laminar sublayer thickness of water and the turbulent boundary layer thickness of air averagely 65%.

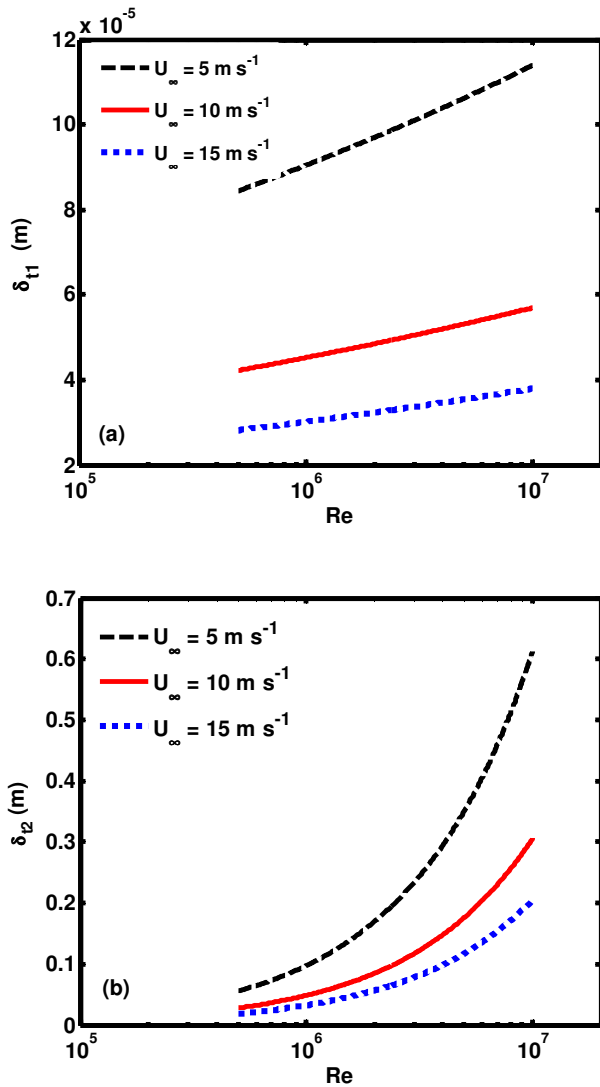


Fig. 3 Influence of the free-stream velocity on (a) the laminar sublayer thickness of water and (b) the turbulent boundary layer thickness of air along the flat plate at $T_w/T_\infty = 5$ and $T_\infty = 25$ °C.

4.3 Influence of wall to free-stream temperature ratio

Figure 4(a) and (b) illustrates influence of wall to free-stream temperature ratio (T_w/T_∞) on the laminar viscous sublayer thickness of air and turbulent boundary layer thickness of water, respectively, along the flat plate at free-stream velocity and temperature of 25 °C and 10 m/s. As shown in Fig. 4(a), the laminar sublayer thickness (also the turbulent boundary layer thickness) increases for air flow as a result of increasing the wall to free-stream temperature ratio. But this trend occurs differently for water flow. With increasing the wall to free-stream temperature ratio, the turbulent boundary layer thickness (also the laminar sublayer thickness) decreases for water flow, as shown in Fig. 4(b). As such, the plate acts as the source of momentum for the flow. The transportation rate of momentum through the air flow rises with the kinematic viscosity of the fluid. Because the kinematic viscosity of gases increases with temperature, the momentum boundary layer thickness increases as well. On the other hand, liquids show the opposite trend in kinematic viscosity variation with temperature. It means that the momentum transportation rate through water flow is reduced as temperature rises.

Figure 4(a) and (b), respectively, show increasing T_w/T_∞ from 2 to 8 leads to increase the laminar sublayer thickness of air nearly 44% and to decrease the turbulent boundary layer thickness of water averagely 60%.

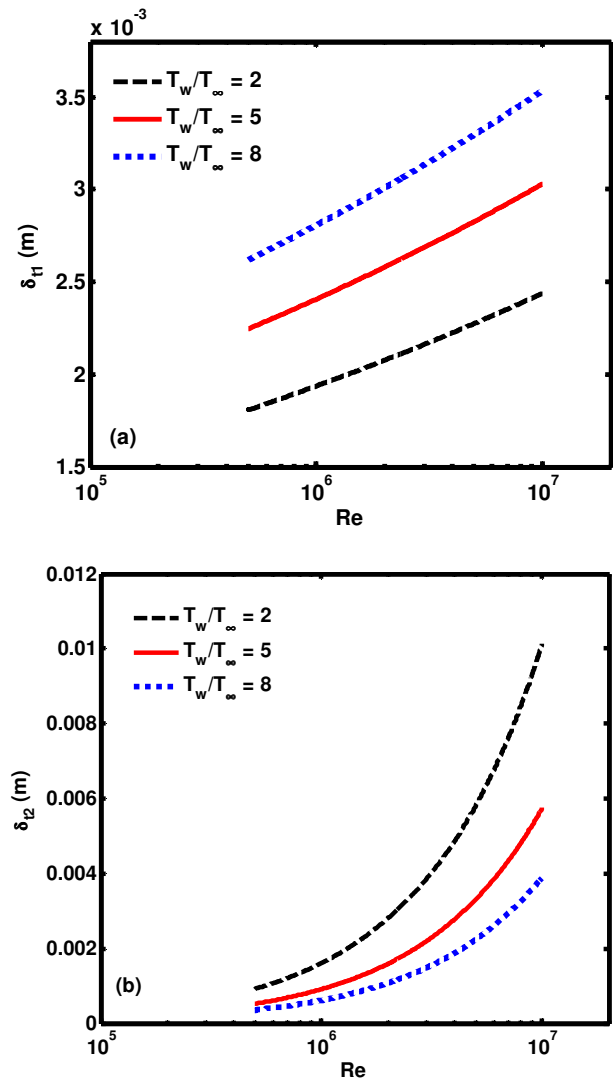


Fig. 4 Influence of T_w/T_∞ on (a) the laminar sublayer thickness of air and (b) the turbulent boundary layer thickness of water along the flat plate at $u_\infty = 10$ m/s and $T_\infty = 25$ °C.

Both comparisons of the results shown by Fig. 3(a) with 4(a) and Fig. 3(b) with 4(b) demonstrate that both laminar sublayer and turbulent boundary layer for water are lower than those for air for the same conditions. For example, at $Re = 10^6$, $T_w/T_\infty = 5$ and free-stream velocity 10 m/s, the laminar sublayer and turbulent boundary layer thicknesses are $\sim 5 \times 10^{-5}$ and 0.001 m for water, respectively, whereas those are $\sim 2.5 \times 10^{-3}$ and 0.05 m for air, respectively. It can be attributed to the fact that the kinematic viscosity of water is quite less than that of air.

4.4 Temperature profile

Figure 5 represents the temperature profile as a function of distance from the wall at $Re = 10^6$, the free-stream velocity and temperature 10 m s⁻¹ and 25 °C, respectively, and $T_w/T_\infty = 5$ for water flow. The temperature decreases with distance from the wall. As can be seen in this figure, in the region near the wall ($y/\delta_{t2} < 0.04$), the temperature profile is linear in the laminar sub-layer zone, and that is a curve line in the fully developed turbulent boundary layer (see Eq. (17)). Also in this figure, temperature profile of this model was compared with the results of $k-\epsilon$ and $k-\omega$ models. The difference between the temperature profile of this model and other models could be due to the approximate nature of the model, choosing the degree of polynomials, or type of temperature profile function.

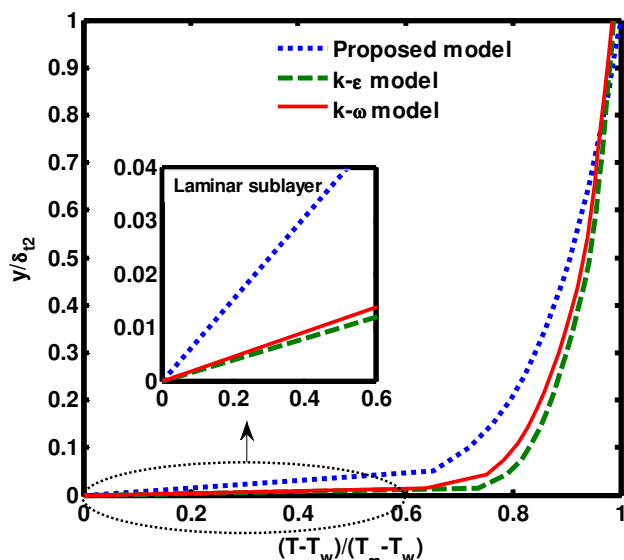


Fig. 5 The temperature profile of water as a function of distance from the wall at $Re = 10^6$, $u_\infty = 10$ m/s, $T_\infty = 25$ °C and $T_w/T_\infty = 5$.

5. CONCLUSIONS

In this study, a new relatively simple turbulent model is proposed to predict the boundary layer thickness and temperature profile in laminar viscous sublayer and fully developed turbulent boundary layer, as well as the heat transfer coefficient for forced convection on a smooth flat plate. The model incorporates the integral energy equations with the polynomial temperature profile. Totally, in addition to the turbulent hydrodynamic boundary layer (Khademi *et al.*, 2010), the thermal boundary layer also grows thicker along the surface of the plate. In addition, some common correlations as well as the $k-\epsilon$, $k-\omega$, RSM models were used to investigate the reliability and accuracy of the proposed model for the cases of air and water flows. The results show that the heat transfer coefficient calculated by the proposed model is in good agreement with the semi-empirical correlations and other established models. Both thermal boundary layers shift to the down with increasing the free-stream velocity. The thermal boundary layer thickness increases for air but that decreases for water with increasing the wall to free-stream temperature ratio.

Finally, the advantages and disadvantages of this new model compared with other established models such as $k-\epsilon$, $k-\omega$, and RSM are as follows: In this model, a set of ODEs have been used to solve the boundary layer problems while, the other models try to estimate turbulence by a set of PDEs. In other word, the other models are very time consuming to solve problems. Therefore, this model is in general much simpler than the other models and easy to use. But it should be noted that, this method is less accurate than other models due to its approximate nature. This model is able to estimate the thickness of laminar sub-layer zone that it may not be possible in other methods.

The results show prediction of turbulence over a smooth flat plate is feasible by this integral energy equation model. The authors are looking to apply this integral model to predict the turbulent flow on the other submerged bodies in future work.

NOMENCLATURE

\bar{v}	Time-smoothed velocity in y direction (m/s)
v'	Fluctuation velocity in y direction (m/s)
T', \bar{u}	Fluctuation temperature and velocity in x direction (K), (m/s)
\bar{T}, \bar{u}	Time-smoothed temperature and velocity in x direction (K), (m/s)
C_p	Heat capacity (J/kg °C)
E_T, E_μ	Eddy thermal conductivity and eddy viscosity (W/m°C), (Pa.s)
h	Heat transfer coefficient (W/m ² °C)
k	Thermal conductivity (W/m °C)
Nu	Nusselt number
Re_x	Reynolds number based on x
T_∞, u_∞	Free-stream temperature and velocity (°C), (m/s)
T_1, u_1	Temperature and velocity in the laminar sub-layer zone (°C), (m/s)
T_2, u_2	Temperature and velocity in the turbulent boundary layer zone (°C), (m/s)
T_w	Wall temperature (°C)
x	Direction along the plate (m)
y	Direction normal to the plate (m)

Greek symbols

μ	Dynamic viscosity (Pa s)
ρ	Density (kg/m ³)
δ^*	Thermal laminar boundary-layer thickness at $Re_{cr}=5 \times 10^5$ (m)
δ_1	Thermal laminar sub-layer thickness (m)
δ_2	Thermal fully developed turbulent boundary-layer thickness (m)
α	Thermal diffusivity (m ² /s)

REFERENCES

- Baehr, H.D., and Stephan, K., 2006, *Heat and Mass Transfer*, 2th ed., Springer, Germany.
- Baldwin, B.S., and Barth, T.J., 1990, "A One-Equation Turbulence Transport Model for High Reynolds Number Wall-Bounded Flows," NASA TM-102847.
- Chung, M.K., and Sung, H.J., 1984, "Four-Equation Turbulence Model for Prediction of the Turbulent Boundary Layer Affected by Buoyancy Force Over a Flat Plate," *International Journal of Heat and Mass Transfer*, **27**(12), 2387-2395.
[http://dx.doi.org/10.1016/0017-9310\(84\)90097-8](http://dx.doi.org/10.1016/0017-9310(84)90097-8)
- Churchill, S.W., 1976, "A Comprehensive Correlating Equation for Forced Convection from Flat Plates," *AIChE Journal*, **22**, 264-268.
<http://dx.doi.org/10.1002/aic.690220207>

Glushko, G., 1965, "Turbulent boundary layer on a flat plate in an incompressible fluid," *Izvestia Akademiyi Nauk SSSR, Mekh*, **4**, 13-20.

Holman, J.P., 1989, *Heat Transfer*, McGraw-Hill, New York.

Ilegbusi, O.J., 1989, "Turbulent Boundary Layer on a Porous Flat Plate with Severe Injection at Various Angles to the Surface," *International Journal of Heat and Mass Transfer*, **32**(4), 761-765.
[http://dx.doi.org/10.1016/0017-9310\(89\)90223-8](http://dx.doi.org/10.1016/0017-9310(89)90223-8)

Ilegbusi, O.J., and Spalding, D.B., 1989, "An Improved Version of the $k-\omega$ Model of Turbulence," *ASME Journal of Heat Transfer*, **107**(1), 63-69.
<http://dx.doi.org/10.1115/1.3247404>

Khademi, M.H., Zeinolabedini Hezave, A., Mowla, D., and Taheri, M., 2010, "A Simple Model for Turbulent Boundary Layer Momentum Transfer on a Flat Plate," *Chemical Engineering & Technology*, **33**(6), 867-877.
<http://dx.doi.org/10.1002/ceat.200900634>

Kondjoyan, A., Péneau, F., and Boisson, H.C., 2004, "Development of Flat-Plate Thermal and Velocity Boundary Layers under Highly Turbulent and Instable Air Flows: Reynolds Numbers Ranging from 8400 to 127000," *International Journal of Thermal Sciences*, **43**(11), 1091-1100.
<http://dx.doi.org/10.1016/j.ijthermalsci.2004.02.024>

Launder, B.E., Reece, G.J., and Rodi, W., 1975, "Progress in the Development of a Reynolds-Stress Turbulent Closure," *Journal of Fluid Mechanics*, **68**(3), 537-566.
<https://doi.org/10.1017/S0022112075001814>

Launder, B.E., and Sharma, B.I., 1974, "Application of the Energy Dissipation Model of Turbulence to the Calculation of Flow Near a Spinning Disc," *Letters in Heat and Mass Transfer*, **1**(2), 131-137.
[http://dx.doi.org/10.1016/0094-4548\(74\)90150-7](http://dx.doi.org/10.1016/0094-4548(74)90150-7)

Launder, B.E., and Spalding, D.B., 1974, "The Numerical Computation of Turbulent Flows," *Computer Methods in Applied Mechanics and Engineering*, **3**(2), 269-289.
[http://dx.doi.org/10.1016/0045-7825\(74\)90029-2](http://dx.doi.org/10.1016/0045-7825(74)90029-2)

Menter, F.R., 1994, "Two-Equation Eddy-Viscosity Turbulence Models for Engineering Applications," *AIAA Journal*, **32**(8), 1598-1605.
<http://dx.doi.org/10.2514/3.12149>

Nee, V.M., and Kovaszny, L.S.G., 1969, "Simple Phenomenological Theory of Turbulent Shear Bows," *Physics of Fluids*, **12**(3), 473-484.
<http://dx.doi.org/10.1063/1.1692510>

Pinson, F., Gregoire, O., Quintard, M., Prat, M., and Simonin, O., 2007, "Modeling of Turbulent Heat Transfer and Thermal Dispersion for Flows in Flat Plate Heat Exchangers," *International Journal of Heat and Mass Transfer*, **50**(7-8), 1500-1515.
<http://dx.doi.org/10.1016/j.ijheatmasstransfer.2006.08.033>

Pitts, D.R., and Sissom, L.E., 1997, *Schaum's Outline of Theory and Problems of Heat Transfer*, 2nd ed., McGraw-Hill, New York.

Popovac, M., Hanjalic, K., 2007, "Compound Wall Treatment for RANS Computation of Complex Turbulent Flows and Heat Transfer," *Flow, Turbulence and Combustion*, **78**, 177-202.
<http://dx.doi.org/10.1007/s10494-006-9067-x>

Prandtl, L., and Angew, Z., 1925, "Bericht Uber Untersuchungen Zur Ausgebildeten Turbulenz," *Zeitschrift für Angewandte Mathematik und Mechanik*, **5**, 136-139.

Radmehr, A., and Patankar, S.V., 2001, "Computation of Boundary Layer Transition using Low-Reynolds-Number Turbulence Models," *Numerical Heat Transfer, Part B*, **39**(6), 525-543.
<http://dx.doi.org/10.1080/10407790152034809>

Sartori, E., 2006, "Convection Coefficient Equations for Forced Air Flow over Flat Surfaces," *Solar Energy*, **80**(9), 1063-1071.
<http://dx.doi.org/10.1016/j.solener.2005.11.001>

Schlichting, H., 1968, *Boundary Layer Theory*, 6th ed., translated by Kestin, J., McGraw-Hill, New York.

Shames, I.H., 2003, *Mechanics of Fluids*, 4th ed., McGraw-Hill, New York.

Spalart, P.R., and Allmaras, S.R., 1994, "A One-Equation Turbulence Model for Aerodynamic Flows," *La Recherche Aeronautique*, **1**, 5-21.

Sucec, J., 2006, "Modern Integral Method Calculation of Turbulent Boundary Layers," *Journal of Thermophysics and Heat Transfer*, **20**(3), 552-557.
<http://dx.doi.org/10.2514/1.16397>

Theories of Turbulence and Variable Turbulent Prandtl Number," *International Journal of Heat and Mass Transfer*, **16**(8), 1547-1563.
[http://dx.doi.org/10.1016/0017-9310\(73\)90183-X](http://dx.doi.org/10.1016/0017-9310(73)90183-X)

Vallejo, A., and Trevino, C., 1990, "Convective Cooling of a Thin Flat Plate in Laminar and Turbulent Flows," *International Journal of Heat and Mass Transfer*, **33**(3), 543-554.
[http://dx.doi.org/10.1016/0017-9310\(90\)90188-Z](http://dx.doi.org/10.1016/0017-9310(90)90188-Z)

Van Driest, E.R., 1956, "On Turbulent Flow Near a Wall," *Journal of the Aeronautical Sciences*, **23**(11), 1007-1011.
<http://dx.doi.org/10.2514/8.3713>

Wassel, A.T., and Catton, I., 1973, "Calculation of Turbulent Boundary Layers over Flat Plates with Different Phenomenology Theories of Turbulence and Variable Turbulent Prandtl Number," *International Journal of Heat and Mass Transfer*, **16**(8), 1547-1563.
[http://dx.doi.org/10.1016/0017-9310\(73\)90183-X](http://dx.doi.org/10.1016/0017-9310(73)90183-X)

Wilcox, D.C., 1988, "Re-Assessment of the Scale-Determining Equation for Advanced Turbulence Models," *AIAA Journal*, **26**(11), 1299-1310.
<http://dx.doi.org/10.2514/3.10041>

Yakhot, V., Orszag, S.A., Thangam, S., Gatski, T.B., and Speziale, C.G., 1992, "Development of Turbulence Models for Shear Flows by a Double Expansion Technique," *Physics of Fluids A*, **4**(7), 1510-1520.
<http://dx.doi.org/10.1063/1.858424>

Zukauskas, A., and Slanciauskas, A., 1987, *Heat Transfer in Turbulent Fluid Flows*, Hemisphere, Washington.

APPENDIX A: CALCULATION OF THE INTEGRAL ENERGY EQUATION IN THE LAMINAR SUBLAYER ZONE

With due attention to Fig. 1, the input mass flow rate through the laminar sublayer zone is

$$\int_0^{\delta_{n1}} \rho u_1 dy \quad (\text{A.1})$$

and the input energy convected through laminar sublayer zone is

$$\rho C_p \int_0^{\delta_{n1}} u_1 T_1 dy \quad (\text{A.2})$$

The output mass flow rate from the laminar sublayer zone is

$$\int_0^{\delta_{n1}} \rho u_1 dy + \frac{d}{dx} \left(\int_0^{\delta_{n1}} \rho u_1 dy \right) dx \quad (\text{A.3})$$

and the output energy convected from the laminar sublayer zone is

$$\rho C_p \int_0^{\delta_{n1}} u_1 T_1 dy + \frac{d}{dx} \left(\rho C_p \int_0^{\delta_{n1}} u_1 T_1 dy \right) dx \quad (\text{A.4})$$

Considering the conservation of mass and the fact that no mass can enter the control volume through the solid wall, the additional mass

flow in Eq. (A.3) over that in Eq. (A.1) must enter through the laminar sublayer from the top zone (fully develop turbulence zone). This mass flow carriers with it an energy in the x direction equal to

$$C_p T_2 \frac{d}{dx} \left(\int_0^{\delta_{t1}} \rho u_1 dy \right) dx \quad (\text{A.5})$$

The net energy flow out of the control volume is therefore

$$\frac{d}{dx} \left(\rho C_p \int_0^{\delta_{t1}} u_1 T_1 dy \right) dx - C_p T_2 \frac{d}{dx} \left(\int_0^{\delta_{t1}} \rho u_1 dy \right) dx \quad (\text{A.6})$$

or

$$\frac{d}{dx} \left(\rho C_p \int_0^{\delta_{t1}} u_1 T_1 dy \right) dx - \rho C_p \frac{d}{dx} \left(\int_0^{\delta_{t1}} u_1 T_2 dy \right) dx + \rho C_p \frac{dT_2}{dx} \left(\int_0^{\delta_{t1}} u_1 dy \right) dx \quad (\text{A.7})$$

The heat transfer at the wall is

$$-k dx \frac{\partial T_1}{\partial y} \Big|_{y=0} \quad (\text{A.8})$$

The heat transfer between the laminar sublayer and the fully developed turbulence zone is

$$-k dx \frac{\partial T_1}{\partial y} \Big|_{y=\delta_{t1}} \quad (\text{A.9})$$

and the viscous-dissipation term within the laminar sublayer zone is

$$\mu \left[\int_0^{\delta_{t1}} \left(\frac{du_1}{dy} \right)^2 dy \right] dx \quad (\text{A.10})$$

Combining these energy quantities according to energy balance equation and collecting terms gives the integral energy equation in the laminar sublayer zone as follows

$$\rho C_p \frac{d}{dx} \int_0^{\delta_{t1}} (T_1 - T_2) u_1 dy + \rho C_p \frac{dT_2}{dx} \Big|_{y=\delta_{t1}} \int_0^{\delta_{t1}} u_1 dy + k \frac{\partial T_1}{\partial y} \Big|_{y=0} - k \frac{\partial T_1}{\partial y} \Big|_{y=\delta_{t1}} - \mu \int_0^{\delta_{t1}} \left(\frac{du_1}{dy} \right)^2 dy = 0 \quad (\text{A.11})$$

APPENDIX B: CALCULATION OF THE INTEGRAL ENERGY EQUATION IN THE FULLY DEVELOP TURBULENCE ZONE

The input mass flow rate through the fully develop turbulence zone is

$$\int_{\delta_{t1}}^{\delta_{t2}} \rho u_2 dy \quad (\text{B.1})$$

and the input energy convected through the fully develop turbulence zone is

$$\rho C_p \int_{\delta_{t1}}^{\delta_{t2}} u_2 T_2 dy \quad (\text{B.2})$$

The output mass flow rate from the fully develop turbulence zone is

$$\int_{\delta_{t1}}^{\delta_{t2}} \rho u_2 dy + \frac{d}{dx} \left(\int_{\delta_{t1}}^{\delta_{t2}} \rho u_2 dy \right) dx \quad (\text{B.3})$$

and the output energy convected from the fully develop turbulence zone is

$$\rho C_p \int_{\delta_{t1}}^{\delta_{t2}} u_2 T_2 dy + \frac{d}{dx} \left(\rho C_p \int_{\delta_{t1}}^{\delta_{t2}} u_2 T_2 dy \right) dx \quad (\text{B.4})$$

Considering the conservation of mass and the output mass flow rate from the fully develop turbulence zone through the laminar sublayer (second term of Eq. (A.3)), the input mass flow rate from the free-stream through the fully develop turbulence zone is obtained. This mass flow carriers with it an energy in the x direction equal to

$$C_p T_\infty \frac{d}{dx} \left(\int_{\delta_{t1}}^{\delta_{t2}} \rho u_2 dy \right) dx + C_p u_\infty \frac{d}{dx} \left(\int_0^{\delta_{t1}} \rho u_1 dy \right) dx \quad (\text{B.5})$$

The net energy flow out of the control volume is therefore

$$\frac{d}{dx} \left(\rho C_p \int_{\delta_{t1}}^{\delta_{t2}} u_2 T_2 dy \right) dx + C_p T_2 \frac{d}{dx} \left(\int_0^{\delta_{t1}} \rho u_1 dy \right) dx - C_p T_\infty \frac{d}{dx} \left(\int_{\delta_{t1}}^{\delta_{t2}} \rho u_2 dy \right) dx - C_p T_\infty \frac{d}{dx} \left(\int_0^{\delta_{t1}} \rho u_1 dy \right) dx \quad (\text{B.6})$$

and the viscous-dissipation term within the fully developed turbulence zone is

$$\left[\int_{\delta_{t1}}^{\delta_{t2}} E_\mu \left(\frac{du_2}{dy} \right)^2 dy \right] dx \quad (\text{B.7})$$

Considering constant free-stream temperature, setting the energy balance equation and collecting terms gives the integral energy equation in the fully develop turbulence zone as follows

$$\rho C_p \frac{d}{dx} \int_{\delta_{t1}}^{\delta_{t2}} (T_2 - T_\infty) u_2 dy + \rho C_p \frac{d}{dx} \int_0^{\delta_{t1}} (T_2 - T_\infty) u_1 dy - \rho C_p \frac{dT_2}{dx} \Big|_{y=\delta_{t1}} \int_0^{\delta_{t1}} u_1 dy + k \frac{\partial T_1}{\partial y} \Big|_{y=\delta_{t1}} - \int_{\delta_{t1}}^{\delta_{t2}} E_\mu \left(\frac{du_2}{dy} \right)^2 dy = 0 \quad (\text{B.8})$$